Kuwait J.Sci., Vol.49, No.(4),October.2022,pp(1-11)

Broadband low-frequency sound absorption via a hexagonal acoustic metamaterial in the honeycomb structure

Fatma Nafaa Gaafer

Dept. of Science, College of Basic Education, Wasit University, Iraq
Corresponding author: fnafie@uowasit.edu.iq

Abstract

I constructed two models for achieving a perfect absorption acoustic metamaterial using a hexagonal honeycomb structure in the air with a change in folding number. The purpose of these models was to construct a hexagonal honeycomb metamaterial derived from Polydimethylsiloxane (PDMS) polymer. I carried out finite element simulations using COMSOL Multiphysics software to take theoretical measurements for our honeycomb structure and to show the influence of structural parameters in our models. Our simulations revealed that, depending upon the theoretical analysis, an acoustic metamaterial that supports resonance at 210 Hz for folding number n = 6 can be developed to construct a low-frequency sound-absorbing technology. I demonstrate that the dissipative loss effect can be controlled by folding number and high space utilization through adjusting the hexagonal dimensions to achieve perfect absorption. I also demonstrate the important effects of folding number, rotation angle, and structural parameters on improving acoustic absorption performance for honeycomb structural design. The results are of extraordinary correspondence at low frequency for achieving an ideal sound absorbing material.

Keywords: Acoustic focusing; acoustic metamaterial; hexagonal honeycomb structure; perfect absorber; sound insulation.

1. Introduction

Acoustic metamaterials (Mei *et al*., 2012) and metasurfaces (Ma *et al*., 2014) have attracted a great deal of work dedicated to designing new materials and structures of deep subwavelength thickness at work frequency in recent years. Acoustic metamaterials have been an important study topic in recent years. Acoustic cloaking, perfect absorbers (Ma *et al*., 2014), Sound concentration based on index lens gradient (Climente *et al*., 2010; Welter *et al*., 2011; Zhao *et al*., 2016), acoustic topological systems (Ni *et al*., 2015; Peano *et al*., 2015; Peng *et al*., 2016), and other applications have been developed. Furthermore, nonlinear acoustic metamaterials have recently received increased interest via research on acoustic diodes (Li *et al*., 2011; Liang *et al*., 2009), bifurcation-based acoustic switching and rectification (Boechler *et al*., 2011), nonlinear acoustic lenses (Donahue *et al*., 2014), and acoustic solitons (Achilleos *et al*., 2015). In other research, linear losses are attributed to low dissipation. However, nonlinear losses may quickly arise in acoustics, for example, due to geometrical discontinuities. Controlling sound waves on a subwavelength scale was challenging in acoustics due to the constraints of the mass law until the discovery of acoustic metamaterials (Li &

Chan, 2004; Li *et al*., 2016; Liu *et al*., 2000; Pennec *et al*., 2008; Yang *et al*., 2008). Artificially constructed acoustic metamaterials contradict the mass rule and exhibit several exceptional and uncommon acoustic characteristics such as negative refraction (Feng *et al*., 2005; Li *et al*., 2016; Mokhtari *et al*., 2019; Nemat-Nasser, 2019; Zhang & Liu, 2004; Zhu *et al*., 2014), acoustic focusing, and remarkable transmission, piquing the attention of many scientists and researchers (Liu *et al*., 2020; Songkaitiwong & Locharoenrat, 2020). In-room acoustics sound absorption is essential (e.g., reduction of noise). In recent decades, the following have been widely explored: Dark-acoustic metamaterials, including such porosity (Biot, 1962) structures (Lee *et al*., 2010; Ma *et al*., 2014), hybrid resonator membrane patterns (Jiang *et al*., 2017; Xiao *et al*., 2015; Zhao *et al*., 2020), metamaterials of plates (Badreddine *et al*., 2012), and resonators of the Helmholtz oscillation (Cai *et al*., 2014). The resonant structures supporting the increasing density of acoustics during resonant frequencies have been highly able to absorb sound (<500 Hz) at low frequency due to the non-trivial wave diffraction of conventional sound-absorber material plastic foam, fiberglass, and mineral wool (Allard & Atalla, 2009). As stated in earlier studies, space coiling may be used to build counterintuitive metamaterials. These metamaterials have a single negative/double negative zero indexes metamaterial and a very high index of refractive metamaterials. These extreme material characteristics are usually complex values in which the imaginary parts indicate the intrinsic loss or absorption of energy. Note that the zigzag or spiral patterns improve absorption by extending the length of the viscous limit. (Xie *et al*., 2020).

This paper investigates the acoustic metamaterial of a honeycomb structure with various designs that cause the optimal acoustic insulation and absorber design using hexagonal honeycomb structure. The use of finite element simulations via COMSOL Multiphysics software to calculate the absorption coefficient of the hexagonal honeycomb metamaterial. To improve the accuracy of the sound absorber. I proposed models by adjusting the internal parameters of the acoustic metamaterial.

2. Result and discussion

The low-frequency sound (<500Hz) attenuation by deep subwavelength thickness absorber (<5cm) is very interesting in noise control techniques. However, the high penetration of low-frequency sound and essential weakness dissipation of common materials has been challenging. The traditional materials for absorption of sound, such as porosity materials, have proved to be efficient in sound absorption at high frequency (>1000 Hz), but with low frequencies limits if the restricted thickness is imposing (Wu *et al*., 2019). As shown in Figures 1(a) and 1(b), the honeycomb structure has a dimension of length L = 188 mm, width w = 164 mm, height h = 80 mm and the hexagonal inscribed in a circle with that radius to be 30 mm, neck width w_1 = 10 mm and inner width w_2 = 8 mm. In theoretical design consisting of air and acoustic metamaterial Polydimethylsiloxane (PDMS) polymer. The air density is 1.21 Kg/m^3, and the Polydimethylsiloxane (PDMS) density is 995 Kg/m^3, while the corresponding sound velocity of the air is 343 m/s and sound velocity of the Polydimethylsiloxane (PDMS) is 1000 m/s. The metamaterials were placed in an aluminium tube with a square cross-section, as presented in Figure 1(c).

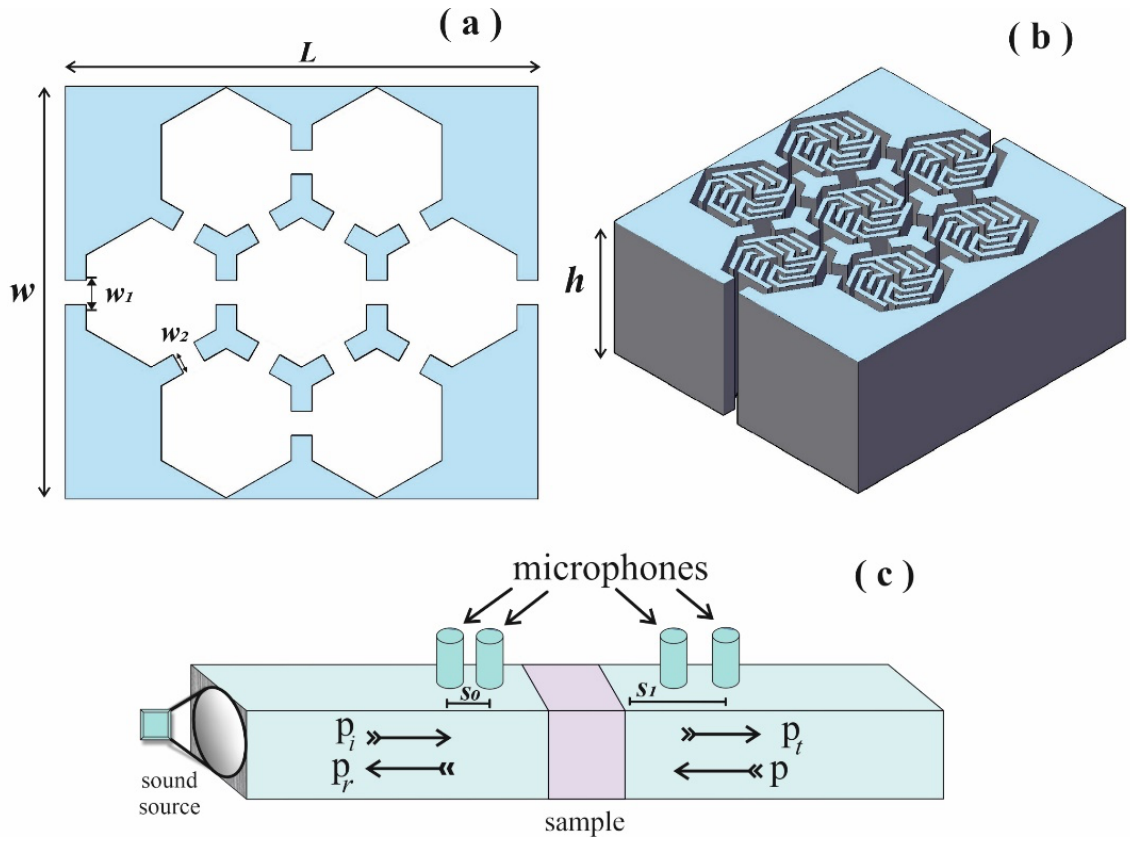

Fig. 1. (a) Schematic diagram of the hexagonal honeycomb structure dimensions without models. (b) Schematic diagram of the hexagonal honeycomb structure with the second model at n = 6. (c) The samples (honeycomb structure) were placed between two Aluminum tubes with a square cross-section, four microphones in the two-port technique, where p, p_t, p_i, p_r, and are the complex amplitudes of the transmitted, incident, and reflected plane waves, respectively.

I carefully designed two models of the absorber acoustic metamaterial of the honeycomb structure constructed based on the folding number, angle of rotation and geometric parameters of the metamaterial that were changed with high space utilization and moderate lateral dimension to match a hexagonal structure dimensions. Figures 2(a) and 2(b) show the schematics of the folding numbers from n = 2 to n = 6. The first model is denoted in Figure 2(a), where the folding number n = 2 at an angle of rotation by 180°. For the folding numbers n = 3 and 4, the inner shape is designed to be less by 75% at an angle of rotation by 120°, 90°, respectively. When the rotation angle by 72° and 60°, respectively, the internal parameters of the model are decreased by around 70% in the designed structure at folding numbers n = 5 and 6, as marked by the arrow in Figure 2(a). Figure 2(b) shows that the inner shape of the second model metamaterial is designed to match the outer hexagonal structure with narrow channels that take the form of hexagonal at the folding number n = 2, 3, and 6 with an angle rotation by 180°, and 120°, respectively. The internal channels hexagonal structure takes the form of a honeycomb lattice.

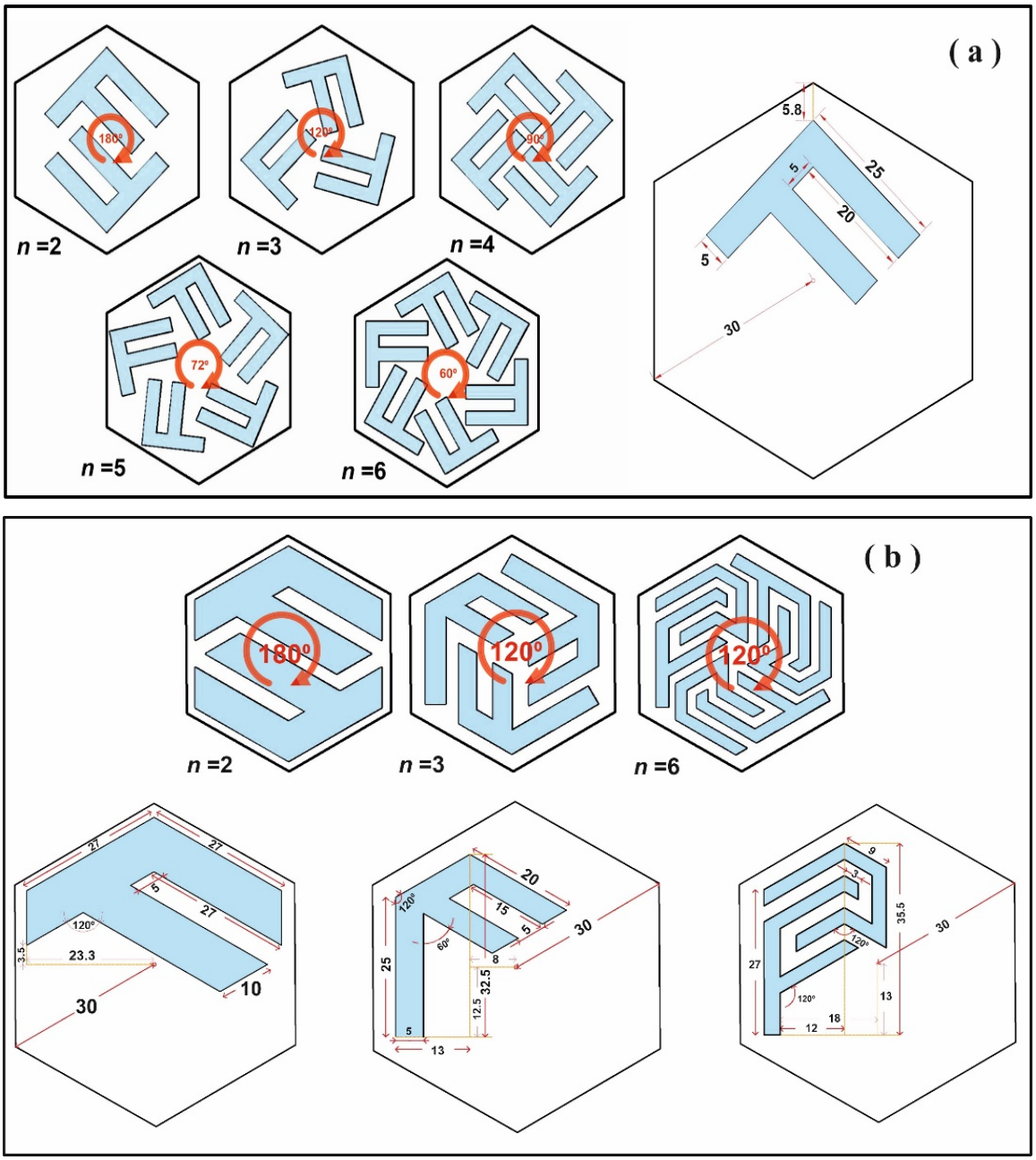

Fig. 2. (a) and (b) Schematic diagram, the hexagonal metamaterial structure with different folding numbers *n*, rotation angle, and geometric parameters.

I employ the COMSOL Multiphysics finite element solver to calculate the acoustic metamaterial simulation absorption coefficient as $A = 1 - |r|^2 - |t|^2$ with r and t representing the reflection and transmission coefficients, respectively. The microphones are placed symmetrically about the sample with the positions, as shown in Figure 1(c). The complex pressures at the measurement positions are then (Mahjoob *et al*., 2009):

$$p_1 = p_i\, e^{ikb_1} + p_r\, e^{-ikb_1} \quad (1)$$

$$p_2 = p_i\, e^{ikb_2} + p_r\, e^{-ikb_2} \quad (2)$$

$$p_3 = p\, e^{ikb_3} + p_t\, e^{-ikb_3} \quad (3)$$

$$p_4 = p\, e^{ikb_4} + p_t\, e^{-ikb_4} \quad (4)$$

The four complex sound pressures can then be obtained from the measurements as

$$p_i = (p_1 \exp(jks_o) - p_2)\exp(-jks_1) \quad (5)$$

$$p_r = (p_2 - p_1 \exp(-jks_o))\exp(jks_1) \quad (6)$$

$$p = (p_4 \exp(jks_o) - p_3)\exp(-jks_1) \quad (7)$$

$$p_t = (p_3 - p_4 \exp(-jks_o))\exp(jks_1) \quad (8)$$

In formula $s_o = b_1 - b_2 = b_4 - b_3$ and $s_1 = b_1 = b_4$ since the microphones are symmetrically placed about the metamaterial slab. where p_t, p_r, and p_i are transmitted, reflected, and incident plane modes, respectively (Feng, 2013). From previous equations, the reflection ($r = p_r / p_i$), and transmission ($t = p_t / p_i$) coefficients are obtained as follows:

$$r = \frac{(p_2 - p_1 \exp(-iks_0))\exp(iks_1)}{(p_1 \exp(iks_0) - p_2)\exp(-iks_1)} \quad (9)$$

$$\mathrm{t} = \frac{(p_3 - p_4 \exp(-jks_o))\exp(jks_1)}{(p_1 \exp(iks_0) - p_2)\exp(-iks_1)} \quad (10)$$

Where s_0 and s_1 are the distance between microphone and sample, respectively, k is the effective wave number for sound waves propagating inside the structure ($k = 2\pi f$/c, where f indicates the frequency in Hz, and c sound velocity of the air is 343 m/s).

If waves travel through the structure of a wave, energy trapped in the resonant element produces a perfect metamaterial absorber. In the first model, I would study the effect of a different folding number with inner shape dimensions of the honeycomb structure to achieve ideal sound absorption. The absorption performance of the absorber is tightly related to its inner meandering paths in the honeycomb structure. The results reveal high space utilization in hexagonal honeycomb structure led to a perfect absorber at the decreased rotation angle in the five cases, as shown in Figure 2(a). Figure 3(a) shows the effect geometric parameters of the absorber with three-folding numbers (n=2, 3, 4) at low-frequency of 209Hz, 242Hz, and 202Hz, respectively. It can be found that the absorption coefficient peak at 0.935, 0.722, and 0.95, respectively. It can be seen that the absorption coefficients peak moves to low frequency, the peak of sound absorption has been improved with the increase of the folding number, and the sound absorber performance of the honeycomb structure with $n = 4$ is better than that of the other two structures. Figures 3(b) and 3(c) compare the sound absorptions for the folding numbers between $n = 5$ and $n = 6$ with low-frequency. Figure 3(b) shows a high absorption peak at a lower frequency by 128.5Hz and 140 Hz

at 0.999 by adjusting the folding number n = 5. From Figure 3(c), the frequency of the sound absorption of the honeycomb structure is 114.5Hz and 124Hz at (0.95) of the absorption coefficient. I further compute the velocity fields in the absorber metamaterial to detect the physical mechanism of acoustic absorption in the structure. Figures 3(d)–3(j) show the simulated particle velocity fields at different frequencies of 209 Hz, 242 Hz, 202 Hz, 128.5Hz, 140 Hz, 114.5Hz and 124Hz, respectively, where the arrows mark the corresponding absorption coefficients in Figures 3(a), 3(b) and 3(c). From simulations, the local resonances play an essential role in the optimal sound absorber, which causes non-trivial relative motion in the viscous boundary layer through resonance-induced velocity fields (Ward *et al*., 2015).

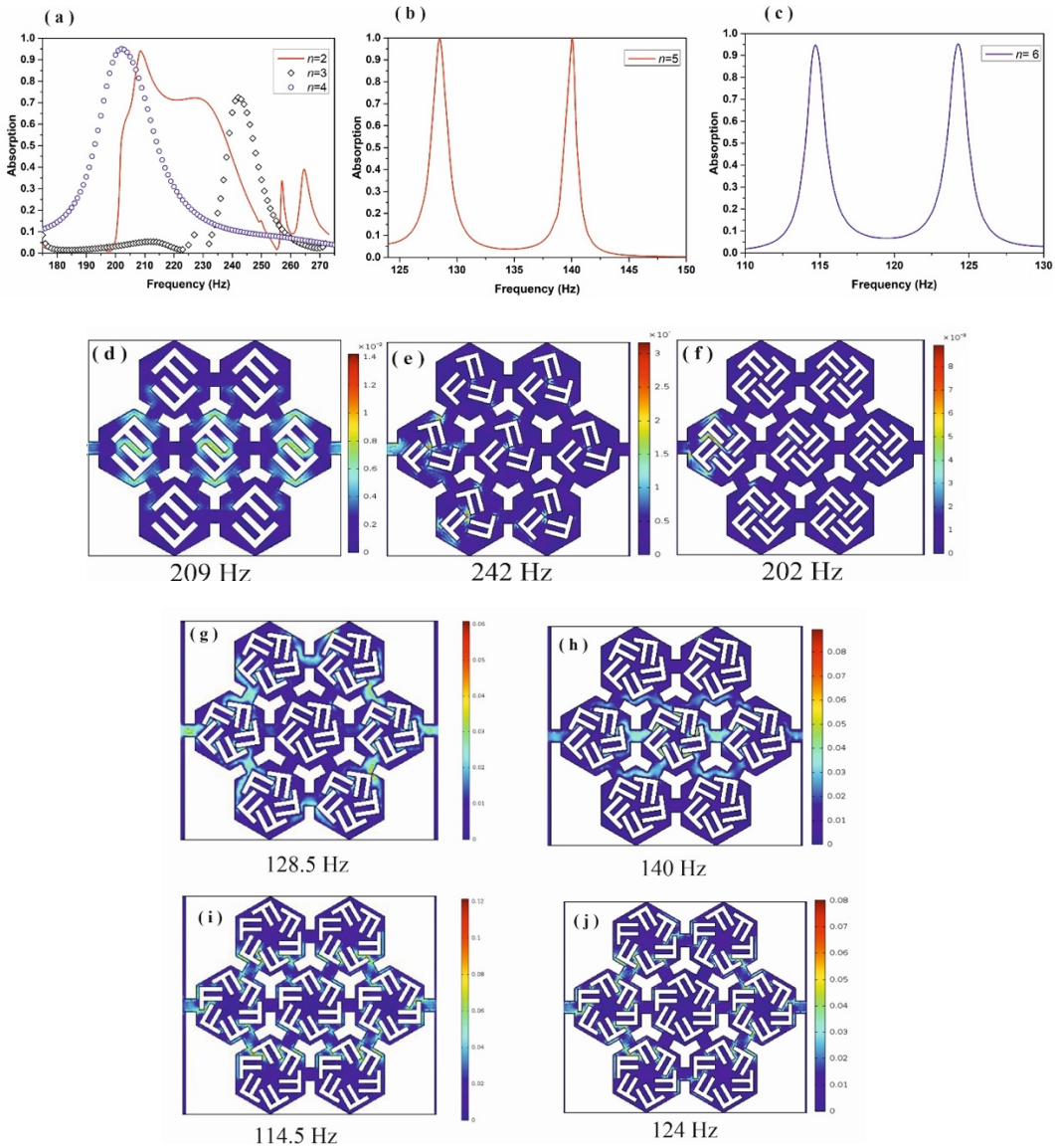

Fig. 3. (a), (b), and (c) Absorption coefficients as frequency function for acoustic metamaterial in the air at different folding numbers n = 2, 3, 4, 5 and 6. (d-j) Simulated particle velocity fields of sound at the frequencies of 209 Hz, 242 Hz, 202 Hz, 128.5Hz, 140 Hz, 114.5Hz, and 124Hz, respectively.

Figures 4(a), 4(b), and 4(c) show that the internal geometric parameters change with designs, as shown in Figure 2(b). Searching for the incident sound waves entering through to honeycomb metamaterial paves the way to achieve the perfect absorber at low-frequency. The incidence wave energy is lost mainly because of the increased friction between the wave and the internal shape of the channels. Therefore, an acoustic absorber low-frequency absorption mechanism converts sound energy resonance frequency into thermal energy. Figure 4(a) and 4(b) shows the absorption coefficient of the absorber. One can observe that the finite element simulation results are 210 Hz and 119.5 Hz at folding numbers (n = 2, 3) with an absorption peak of 0.982 and 0.81, respectively, and almost perfect absorption is obtained. Due to the severe air resonance in the wave structure, the absorption peak is generated, and after that, the sound energy is dissipated mainly by the loss of friction and viscous damping. The absorption coefficient set by n shows that the metamaterials enable to slow down the effective speed of acoustic waves due to path elongation through folded narrow channels. Unitary sound absorption is seen at 210 Hz for n = 6, i.e., absorption peaks are substantially increased at low frequencies while n increases, as shown in Figure 4(c). In Figure 4(d) - 4(f), I further show the particle velocity fields at the rotation angles of 180° and 120°, with the frequencies at 210 Hz, 119.5Hz, and 210 Hz, respectively. The results reveal that at the operating frequencies for the three cases, local resonances take place with non-trivial particle velocity fields observed at the rotation angles, leading to perfect sound absorption. It provides two critical guidelines for the application of acoustic metamaterial devices. Firstly, the maximum intensity of absorption is affected by n and also the internal geometric parameters. The other is that the effective length of the hexagonal structure of the internal channels primarily affects the optimum absorption.

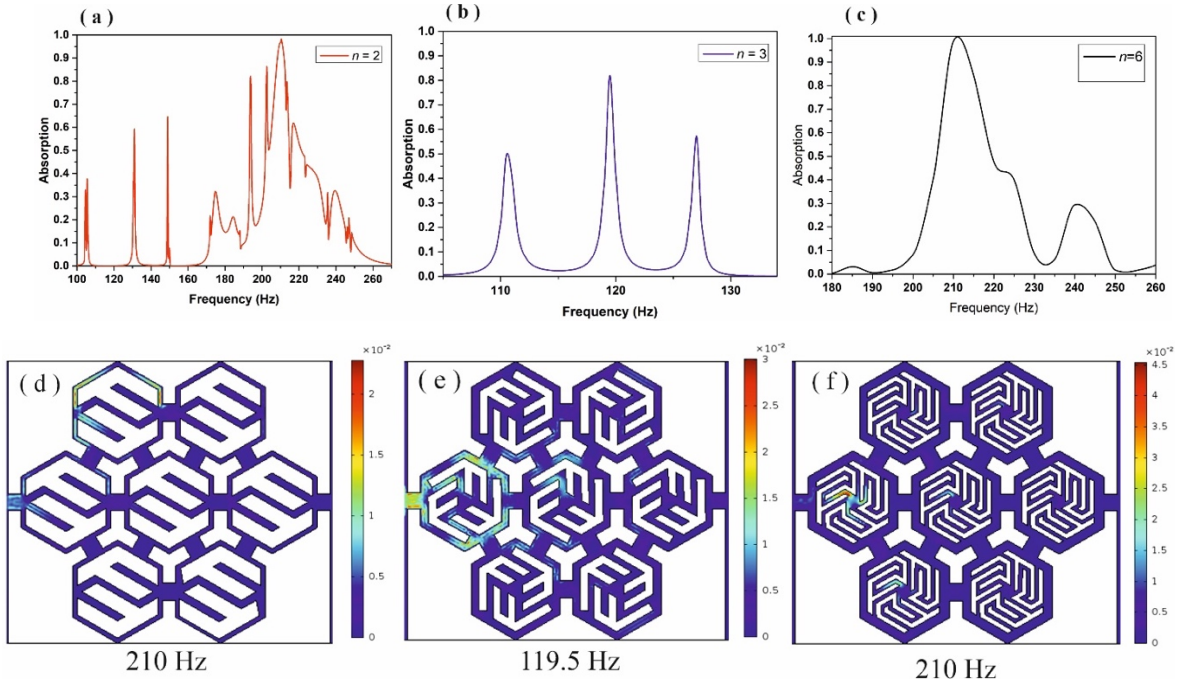

Fig. 4. (a), (b), and (c) Absorption coefficients as frequency function for acoustic metamaterial in the air at different folding numbers n = 2, 3, and 6. (d-f) Simulated particle velocity fields of sound at the frequencies of 210 Hz, 119.5 Hz, and 210Hz, respectively.

3. Conclusion

A finite element simulation of the acoustic metamaterial composed hexagonal honeycomb structure with different folding numbers *n* for two models are developed using multi-physics commercial software COMSOL. Therefore, metamaterial structures for satisfying the perfect absorption at low frequency in the air are designed. I focus on the concept of hexagonal honeycomb metamaterial with changes in shapes dimensions and folding numbers to match hexagonal structure dimensions. A theory of the perfect absorber of hexagonal honeycomb metamaterial is proposed. This feature was exploited for low-frequency acoustic absorbers, which play an essential role in sound absorption in honeycomb metamaterial containing the influence of structural parameters and effective length of the hexagonal structure of the internal channels that could be detected for achieving higher absorption. At the frequency of resonance 210 Hz, the effect of sound-absorbing in the second model material is reached 99%. The friction loss and viscous damping of sound energy contribute extremely to better performance related to the sound-absorbing of this metamaterial.

References

Achilleos, V., Richoux, O., Theocharis, G., & Frantzeskakis, D. J. (2015). Acoustic solitons in waveguides with Helmholtz resonators: Transmission line approach. Physical Review E - Statistical, Nonlinear, and Soft Matter Physics, 91(**2**).

Allard, J. F., & Atalla, N. (2009). Propagation of Sound in Porous Media: Modelling Sound Absorbing Materials. Propagation of Sound in Porous Media: Modelling Sound Absorbing Materials, 1–358. https://doi.org/10.1002/9780470747339

Badreddine Assouar, M., Senesi, M., Oudich, M., Ruzzene, M., & Hou, Z. (2012). Broadband plate-type acoustic metamaterial for low-frequency sound attenuation. Applied Physics Letters, 101(**17**). https://doi.org/10.1063/1.4764072

Biot, M. A. (1962). Generalized Theory of Acoustic Propagation in Porous Dissipative Media. The Journal of the Acoustical Society of America, 34(**9A**), 1254–1264.

Boechler, N., Theocharis, G., & Daraio, C. (2011). Bifurcation-based acoustic switching and rectification. Nature Materials, 10(**9**), 665–668. https://doi.org/10.1038/nmat3072

Cai, X., Guo, Q., Hu, G., & Yang, J. (2014). Ultrathin low-frequency sound absorbing panels based on coplanar spiral tubes or coplanar Helmholtz resonators. Applied Physics Letters, 105(**12**). https://doi.org/10.1063/1.4895617

Climente, A., Torrent, D., & Sánchez-Dehesa, J. (2010). Sound focusing by gradient index sonic lenses. Applied Physics Letters, 97(**10**). https://doi.org/10.1063/1.3488349

Donahue, C. M., Anzel, P. W. J., Bonanomi, L., Keller, T. A., & Daraio, C. (2014). Experimental realization of a nonlinear acoustic lens with a tunable focus. Applied Physics Letters, 104(**1**). https://doi.org/10.1063/1.4857635

Feng, Leping. (2013). Modified impedance tube measurements and energy dissipation inside absorptive materials. Applied Acoustics, 74(**12**), 1480–1485.

Feng, Liang, Liu, X. P., Chen, Y. Bin, Huang, Z. P., Mao, Y. W., Chen, Y. F., Zi, J., & Zhu, Y. Y. (2005). Negative refraction of acoustic waves in two-dimensional sonic crystals. Physical Review B - Condensed Matter and Materials Physics, 72(**3**).

Jiang, X., Li, Y., & Zhang, L. (2017). Thermoviscous effects on sound transmission through a metasurface of hybrid resonances. The Journal of the Acoustical Society of America, 141(**4**), EL363–EL368. https://doi.org/10.1121/1.4979682

Lee, S. H., Park, C. M., Seo, Y. M., Wang, Z. G., & Kim, C. K. (2010). Composite acoustic medium with simultaneously negative density and modulus. Physical Review Letters, 104(**5**). https://doi.org/10.1103/PhysRevLett.104.054301

Li, Jensen, & Chan, C. T. (2004). Double-negative acoustic metamaterial. Physical Review E - Statistical Physics, Plasmas, Fluids, and Related Interdisciplinary Topics, 70(**5**), 4. https://doi.org/10.1103/PhysRevE.70.055602

Li, Junfei, Zhou, X., Huang, G., & Hu, G. (2016). Acoustic metamaterials capable of both sound insulation and energy harvesting. Smart Materials and Structures, 25(**4**).

Li, X. F., Ni, X., Feng, L., Lu, M. H., He, C., & Chen, Y. F. (2011). Tunable unidirectional sound propagation through a sonic-crystal-based acoustic diode. Physical Review Letters, 106(**8**). https://doi.org/10.1103/PhysRevLett.106.084301

Liang, B., Yuan, B., & Cheng, J. C. (2009). Acoustic diode: Rectification of acoustic energy flux in one-dimensional systems. Physical Review Letters, 103(**10**).

Liu, Y., Xu, W., Chen, M., Yang, T., Wang, K., Huang, X., Jiang, H., & Wang, Y. (2020). Three-dimensional fractal structure with double negative and density-near-zero properties on a subwavelength scale. Materials and Design, 188. https://doi.org/10.1016/j.matdes.2020.108470

Liu, Z., Zhang, X., Mao, Y., Zhu, Y. Y., Yang, Z., Chan, C. T., & Sheng, P. (2000). Locally resonant sonic materials. Science, 289(**5485**), 1734–1736.

Ma , G., Yang, M., Xiao, S., Yang, Z., & Sheng, P. (2014). Acoustic metasurface with hybrid resonances. Nature Materials, 13(**9**), 873–878. https://doi.org/10.1038/nmat3994

Mahjoob, M. J., Mohammadi, N., & Malakooti, S. (2009). An investigation into the acoustic insulation of triple-layered panels containing Newtonian fluids: Theory and experiment. Applied Acoustics, 70(**1**), 165–171. https://doi.org/10.1016/j.apacoust.2007.12.002

Mei , J., Ma, G., Yang, M., Yang, Z., Wen, W., & Sheng, P. (2012). Dark acoustic metamaterials as super absorbers for low-frequency sound. Nature Communications, 3.

Mokhtari, A. A., Lu, Y., & Srivastava, A. (2019). On the emergence of negative effective density and modulus in 2-phase phononic crystals. Journal of the Mechanics and Physics of Solids, 126, 256–271. https://doi.org/10.1016/j.jmps.2019.02.016

Nemat-Nasser, S. (2019). Inherent negative refraction on acoustic branch of two dimensional phononic crystals. Mechanics of Materials, 132(**4**), 1–8.

Ni, X., He, C., Sun, X. C., Liu, X. P., Lu, M. H., Feng, L., & Chen, Y. F. (2015). Topologically protected one-way edge mode in networks of acoustic resonators with circulating air flow. New Journal of Physics, 17. https://doi.org/10.1088/1367-2630/17/5/053016

Peano, V., Brendel, C., Schmidt, M., & Marquardt, F. (2015). Topological phases of sound and light. Physical Review X, 5(**3**). https://doi.org/10.1103/PhysRevX.5.031011

Peng, Y. G., Qin, C. Z., Zhao, D. G., Shen, Y. X., Xu, X. Y., Bao, M., Jia, H., & Zhu, X. F. (2016). Experimental demonstration of anomalous Floquet topological insulator for sound. Nature Communications, 7. https://doi.org/10.1038/ncomms13368

Pennec, Y., Djafari-Rouhani, B., Larabi, H., Vasseur, J. O., & Hladky-Hennion, A. C. (2008). Low-frequency gaps in a phononic crystal constituted of cylindrical dots deposited on a thin homogeneous plate. Physical Review B - Condensed Matter and Materials Physics, 78(**10**).

Songkaitiwong, K., & Locharoenrat, K. (2020). Computational algorithm of high-intensity focused ultrasound beams in cancer tissue model for hyperthermia therapy. Kuwait Journal of Science, 47(**1**), 50–64.

Ward, G. P., Lovelock, R. K., Murray, A. R. J., Hibbins, A. P., Sambles, J. R., & Smith, J. D. (2015). Boundary-Layer Effects on Acoustic Transmission Through Narrow Slit Cavities. Physical Review Letters, 115(**4**). https://doi.org/10.1103/PhysRevLett.115.044302

Welter, J. T., Sathish, S., Christensen, D. E., Brodrick, P. G., Heebl, J. D., & Cherry, M. R. (2011). Focusing of longitudinal ultrasonic waves in air with an aperiodic flat lens. The Journal of the Acoustical Society of America, 130(**5**), 2789–2796. https://doi.org/10.1121/1.3640841

Wu, F., Xiao, Y., Yu, Di., Zhao, H., Wang, Y., & Wen, J. (2019). Low-frequency sound absorption of hybrid absorber based on micro-perforated panel and coiled-up channels. Applied Physics Letters, 114(**15**). https://doi.org/10.1063/1.5090355

Xiao, S., Ma, G., Li, Y., Yang, Z., & Sheng, P. (2015). Active control of membrane-type acoustic metamaterial by electric field. Applied Physics Letters, 106(**9**). https://doi.org/10.1063/1.4913999

Xie, S. H., Fang, X., Li, P. Q., Huang, S., Peng, Y. G., Shen, Y. X., Li, Y., & Zhu, X. F. (2020). Tunable Double-Band Perfect Absorbers via Acoustic Metasurfaces with Nesting Helical Tracks. Chinese Physics Letters, 37(**5**). https://doi.org/10.1088/0256-307X/37/5/054301

Yang, Z., Mei, J., Yang, M., Chan, N. H., & Sheng, P. (2008). Membrane-type acoustic metamaterial with negative dynamic mass. Physical Review Letters, 101(**20**).

Zhang, X., & Liu, Z. (2004). Negative refraction of acoustic waves in two-dimensional phononic crystals. Applied Physics Letters, 85(**2**), 341–343. https://doi.org/10.1063/1.1772854

Zhao, H., Wang, Y., Yu, D., Yang, H., Zhong, J., Wu, F., & Wen, J. (2020). A double porosity material for low frequency sound absorption. Composite Structures, 239.

Zhao, J., Bonello, B., & Boyko, O. (2016). Focusing of the lowest-order antisymmetric Lamb mode behind a gradient-index acoustic metalens with local resonators. Physical Review B, 93(**17**). https://doi.org/10.1103/PhysRevB.93.174306

Zhu, R., Liu, X. N., Hu, G. K., Sun, C. T., & Huang, G. L. (2014). Negative refraction of elastic waves at the deep-subwavelength scale in a single-phase metamaterial. Nature Communications, 5. https://doi.org/10.1038/ncomms6510

Submitted: 18/09/2021
Revised: 19/12/2021
Accepted: 26/12/2021
DOI: 10.48129/kjs.16701